

Super-stretchable metallic interconnects on polymer with a linear strain of up to 100%

Yeasir Arafat, Indranath Dutta, and Rahul Panat^{a)}

School of Mechanical and Materials Engineering, Washington State University, Pullman, Washington 99163, USA

(Received 29 April 2015; accepted 14 August 2015; published online 28 August 2015)

Metal interconnects in flexible and wearable devices are heterogeneous metal-polymer systems that are expected to sustain large deformation without failure. The principal strategy to make strain tolerant interconnect lines on flexible substrates has comprised of creating serpentine structures of metal films with either in-plane or out-of-plane waves, using porous substrates, or using highly ductile materials such as gold. The wavy and helical serpentine patterns preclude high-density packing of interconnect lines on devices, while ductile materials such as Au are cost prohibitive for real world applications. Ductile copper films can be stretched if bonded to the substrate, but show high level of cracking beyond few tens of % strain. In this paper, we demonstrate a material system consisting of Indium metal film over an elastomer (PDMS) with a discontinuous Cr layer such that the metal interconnect can be stretched to extremely high linear strain (up to 100%) without any visible cracks. Such linear strain in metal interconnects exceeds that reported in literature and is obtained without the use of any geometrical manipulations or porous substrates. Systematic experimentation is carried out to explain the mechanisms that allow the Indium film to sustain the high strain level without failure. The islands forming the discontinuous Cr layer are shown to move apart from each other during stretching without delamination, providing strong adhesion to the Indium film while accommodating the large strain in the system. The Indium film is shown to form surface wrinkles upon release from the large strain, confirming its strong adhesion to PDMS. A model is proposed based upon the observations that can explain the high level of stretch-ability of the Indium metal film over the PDMS substrate. © 2015 AIP Publishing LLC. [<http://dx.doi.org/10.1063/1.4929605>]

The proliferation of ‘smart’ wearable devices is predicted to lead to the “Internet of Things” (IoT) revolution over the next two decades. The examples of such devices include flexible displays,^{1–4} robotic skin,⁵ stretchable circuits,⁶ hemispherical electronic eye,⁷ epidermal electronics,⁸ cardiac sensors, and diagnostic contact lens.⁹ Flexible electronic platforms typically require that its components be connected with each other on a flexible substrate using metallic interconnects. The design and manufacturing of such interconnects that have high spatial density and can be reliably stretched to large strains has become one of the most critical challenges for the IoT revolution. The essential requirements for the interconnect system include strain compatibility of components at the interfaces, minimal increase in resistivity under stretching, and recovery of the resistivity once the strain is released. In addition, any geometrical manipulation to accommodate deformation must be compatible with the interconnect density demanded by the industry.^{10,11} The current methods to improve interconnect stretch-ability include creating serpentine structures of metal films^{12–20} or non-planar buckling structures.^{21–24} However, thin Cu films often delaminate from polymers during straightening of the serpentine.^{18,19,25,26} Furthermore, Cu films on polyimide show severe cracking at strains above ~20%, even when strongly bonded to the substrate.²⁷ Thin Au films on elastomers have been stretched in excess of 20% when the metal-substrate

interface is intact,^{28–31} but for many applications Au is prohibitively expensive. In general, thin films on elastomers may be stretched somewhat beyond their bulk counterparts due to suppression of necking instability.^{27,32–34} A porous elastomer substrate may also enhance the stretch-ability of metal films,³⁵ although such substrates are not being considered in the electronics industry.

In the current work, we demonstrate a material system with interconnect stretch-ability of the interconnect film with linear strain close to 100% without failure. The system includes Indium over PDMS, with a discontinuous interlayer of Cr. The failure occurs in PDMS unrelated to the Indium film, indicating that the interconnect stretch-ability obtained in the current work is limited by that of the substrate. The mechanisms that allow such a high stretch-ability are shown to include the high plastic deformation of Indium and the movement of the cracked Cr islands during stretching.

Indium was used as the interconnect material since it has a low tensile yield strength (0.8–1.19 MPa) and high ductility (50–70%) at a strain rate of $9 \times 10^{-5} \text{ s}^{-1}$ at room temperature.³⁶ It should also be noted that it creeps rapidly and also recrystallizes at room temperature, potentially relieving the interconnect stress. Polydimethylsiloxane (PDMS) was chosen as the substrate material because of its high deformability, chemical stability, and biocompatibility. PDMS was prepared using Sylgard 184 Silicone Elastomer Kit with the elastomer and the curing agent (10:1 ratio by weight, respectively) were thoroughly mixed using a stirrer, followed by 20 min of debubbling (Cole-Parmer Ultrasonic Bath) and

^{a)} Author to whom correspondence should be addressed. Electronic mail: Rahul.panat@wsu.edu

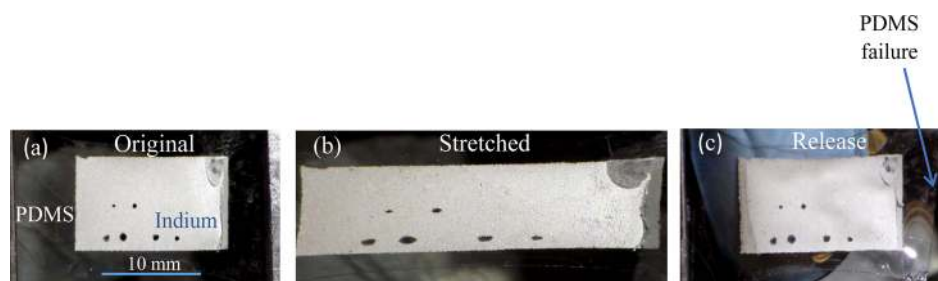


FIG. 1. A $6\ \mu\text{m}$ thick Indium film on a $\sim 0.30\ \text{mm}$ thick PDMS substrate (a) before stretching, (b) loaded to $\sim 91\%$ strain, (c) after failure of the substrate (unrelated to the Indium film). The Indium film shows no indication of external cracking throughout the experiment. (Multimedia view) [URL: <http://dx.doi.org/10.1063/1.4929605.1>]

curing for 3 h at $80\ ^\circ\text{C}$. The PDMS surface was treated with 100 W atmospheric oxygen plasma for 1 min (Surfx Atomflo 400). Large PDMS blocks ($0.30\ \text{mm}$ thick) were prepared and cut into a planar dog-bone shape to facilitate stretching. A thin layer of Cr ($3\text{--}5\ \text{nm}$) followed by an Indium film of about $1\ \mu\text{m}$ thickness was deposited using magnetron sputtering (BOC Edwards Auto 306) at ambient chamber-temperature, without actively heating or cooling the substrate. The sputtered In film served as a seed-layer and provided electrical continuity for subsequent electrodeposition of In on the discontinuous (i.e., cracked) Cr film. Indium film of about $5\ \mu\text{m}$ was then electroplated using an Indium Sulfamate bath (Indium Corporation, USA). The total thickness of the Indium was confirmed using a scanning white light interferometer (Zygo NewView 6300). The Indium film was deposited in a rectangular pattern with a length of about $17.5\ \text{mm}$ and a width of about $9\ \text{mm}$. The choice of the Indium thickness was driven by the requirements of the microelectronics industry.¹¹ Electroplating was conducted at room temperature. The PDMS samples were of dog-bone geometry with the metal film at the center, as shown in Figure 1. The samples were stretched at a constant displacement rate of $\sim 0.035\ \text{mm/s}$, which is equivalent to a strain rate of $\sim 1.3 \times 10^{-3}\ \text{s}^{-1}$ on In film. The strain values correspond to the linear strain in the Indium film and were verified by the location of the fiducial marks on the Indium film surface during stretching. The resistance of the film was measured *in situ* during testing by the 4-wire method.

Figure 1 shows images of Indium on PDMS when the PDMS is stretched (a, b) and after breakage of the sample (c). Ink markers on the film were used to directly measure the strain experienced by the film. The maximum strain obtained in Fig. 1 is about 91% . A total of 17 samples were tested to failure. The strain to failure obtained had a mean of 79.1% and a standard deviation of 9.09% . The maximum strain value obtained was 106% . The failure occurred in the PDMS rather than in the film in all cases. See supplemental material³⁷ for a sample image after failure (Figure S1), a histogram of strain-to-failure data (Figure S2), and a video of the stretching of one of the samples. During stretching, existing defects such as micro-cracks and pinholes appeared to enlarge, but collapsed following unloading. No obvious signs of permanent cracking were observed.

Since volume is conserved during plastic deformation,³⁸ the film resistance increases due to increase in the film length and the resulting decrease in the cross section area. If the film forms defects (e.g., micro-cracks), there is an additional increase in the resistance. The resistivity, ρ also increases due to both plasticity and defects, and is given by

$$\frac{\rho}{\rho_o} = \frac{R}{R_o} \left(\frac{L_o}{L} \right)^2, \quad (1)$$

where ρ_o , L_o , and R_o are the initial values of resistivity, conductor length and resistance, and ρ , L , and R are the instantaneous values of the same quantities, respectively. Here, ρ represents the effective resistivity, and any deviation of ρ/ρ_o from unity represents the combined effects of plasticity and defect formation. Figure 2(a) shows the resistance and resistivity changes of an Indium film during stretching to about 90% , which led to failure of the PDMS outside the Indium film. For the sample in Fig. 2(a), the resistance rises to about 6 times the initial value, whereas the resistivity climbs to about 1.7 times. The rise in resistivity clearly suggests plastic deformation, and possibly, some damage accumulation. However, after a strain of about 30% , the leveling of the resistivity curve despite continued plasticity suggests that there are ongoing recovery processes that limit the growth of resistivity-enhancing dislocations and other defects. Figures 2(b) and 2(c) show the resistance and resistivity changes during 2 complete loading-unloading cycles for a sample that was stretched to $\sim 80\%$. Since abrupt failure of the PDMS results in detachment/movement of the electrical leads,

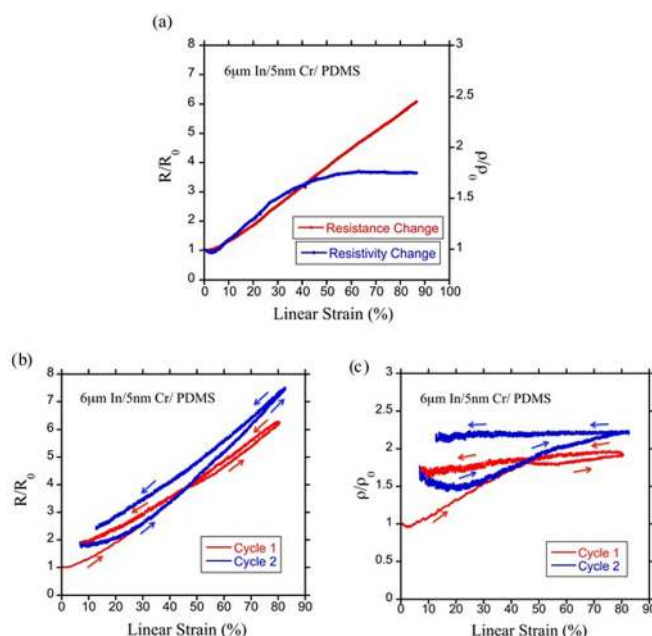


FIG. 2. (a) The change in the resistance of the film and the relative increase in film resistivity for an Indium film on PDMS (with a discontinuous Cr inter-layer) stretched to about 90% strain. (b) Relative change in resistance for two cycles of *in situ* loading and unloading on an Indium film over PDMS up to $\sim 80\%$ film strain. (c) Resistivity change for the cycled sample shown in (b).

resistance measurements during cycling were conducted on samples loaded to well below the substrate fracture strain. Furthermore, since PDMS undergoes significant inelastic extension, the substrate sags (i.e., curves) instead of contracting when the tensile-grip separation approaches that equivalent to zero strain. As a result, the samples were not unloaded below $\sim 5\%$ strain during cycling. It is observed that during elastic deformation during initial loading, R/R_o and ρ/ρ_o remain roughly constant, followed by an increase as plasticity begins. As observed in Fig. 2(a), a slope-change is seen in the resistivity curve around a strain of 30%. This suggests that either recovery or dynamic recrystallization limits the growth of dislocation density, or that further plasticity is concentrated near expanding defects (e.g., micro-cracks), which limits the increase of plastic strain in the rest of the film. Both cycles result in hysteresis of R/R_o and ρ/ρ_o , with net increases in both R and ρ following each cycle. It is noted that during the initial part of the second cycle, resistivity does not rise, since elongation occurs by straightening of wrinkles on the film instead of by plasticity. The formation of wrinkles will be discussed subsequently. However, once the wrinkles are straightened, ρ/ρ_o rises at the same rate as in the first cycle, but without showing the relief due to recovery at larger strains. The cause of this effect, which has been observed in multiple samples, is not understood and needs further investigation. The unloading curves during both cycles have very similar slopes, since the dislocation density induced during loading remains unchanged during unloading.

The strain induced in this work is substantially larger than the strain to fracture of bulk Indium,³⁶ suggesting a mechanism that suppresses strain localization, thereby inhibiting necking and failure of the film. To shed light on this mechanism, we deposited a Cr film of about 3–5 nm thicknesses on the PDMS. The as-deposited Cr film showed

irregular channel cracks as shown in Figure 3(a). Cracking of Cr films deposited on the elastomer substrates has been observed before,^{31,33} and in this instance, can be attributed to *in-situ* heating during deposition, coupled with the much greater thermal expansion coefficient of the underlying substrate, which places the Cr in biaxial tension³⁷ as it is being deposited. The distance between the cracks is about 2–10 μm , while that for cracks with larger spacing is about 20–100 μm .

The PDMS with overlying Cr film was then stretched up to about 39% strain and the same location was imaged under an optical microscope to observe if additional cracks are formed and/or the existing channel cracks widen. The optical images of the cracks at different strain are shown in Figures 3(a)–3(c), respectively, for in-plane loading in the horizontal direction. Clearly, the distance between the Cr islands has increased during elongation. Fig. 3(c) shows wrinkles in the direction perpendicular to the loading, indicating a contraction in the normal direction due to the Poisson effect. Figure 3(d) shows the same location after relaxation from $\sim 39\%$ strain. Comparing Figs. 3(a) and 3(d), it is clear that the Cr does not show significantly large amount of additional cracking (a comparison of Figs. 3(a) and 3(d) reveal only a few new cracks normal to the loading direction). Further, no evidence of delamination of the Cr from PDMS is noted. This demonstrates that Cr remains well bonded to PDMS throughout the experiment, and that widening of the existing Cr-cracks enables the PDMS to be stretched to a large strain.

Under large strain (Fig. 1(b)), the Indium film is expected to have undergone elastic-plastic deformation, while the PDMS elastomer is expected to be under elastic, viscoelastic, and plastic deformation. Upon release, the elastic and viscoelastic recovery of the PDMS are expected to be much higher than those for the Indium. Such inherent incompatibility of a relatively stiff elastic film and a compliant

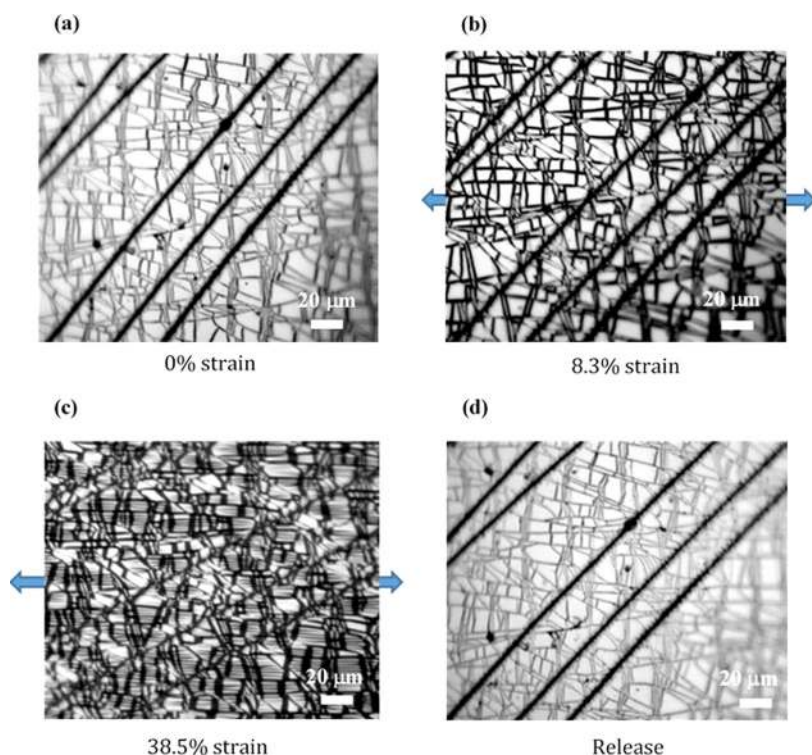


FIG. 3. Microscopic images of cracked Cr layer ($\sim 3\text{--}5$ nm) on Plasma Treated PDMS under different strain levels. The stretching was done for in-plane loading in horizontal direction. (a) Before stretching (b) at 8.3% strain (c) at 38.5% strain and (d) strain released state. The images were taken under same locations so as to spot additional visible changes to the surface while under strain and after releasing strain. Comparing the images before and after strain, it indicates that Cr does not form significantly higher amount of extra cracks.

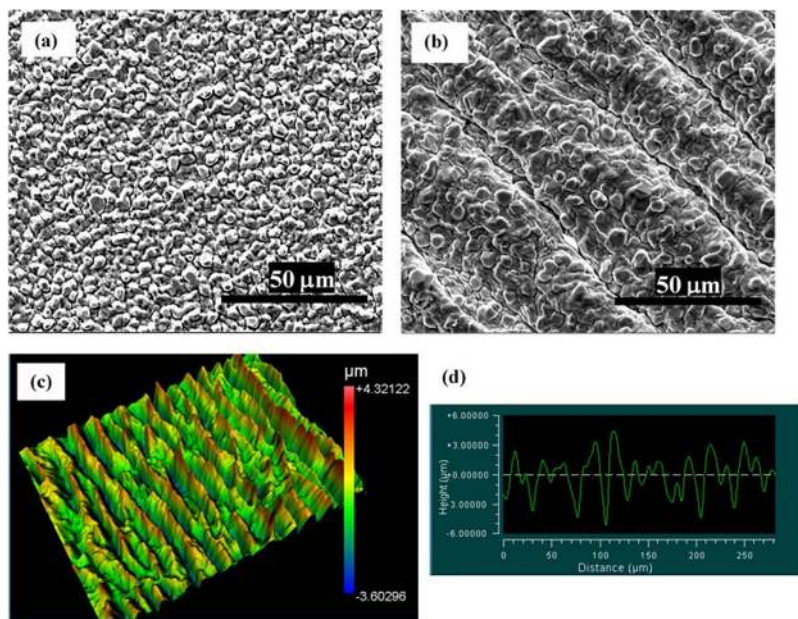


FIG. 4. SEM images of deposited metal film before (a) and after (b) stretching from maximum strain. (c) Optical Profilometer image (Zygo Newview) of about $280 \times 210 \mu\text{m}$ size. (d) Height vs Distance graph at different points on the film surface. The wrinkles formed normal to the loading direction produces wavelength of $18\text{--}20 \mu\text{m}$ and amplitude of $2\text{--}4 \mu\text{m}$.

elastomer is well documented and results in the formation of surface wrinkles.³⁹ Figure 4 shows the SEM micrograph of the film prior to stretching (Fig. 4(a)) and after release (Fig. 4(b)) from maximum strain. Fig. 4(a) shows the as-deposited Indium surface with columnar grains of $2.5\text{--}3.5 \mu\text{m}$ diameter. Upon stretching to about 100% strain and subsequent release, the Indium film has formed wrinkles perpendicular to the loading direction, as seen in the SEM micrograph of Fig. 4(b). The surface profile of a region about $280 \times 210 \mu\text{m}$ in area is shown in Fig. 4(c), where the wrinkles are clearly evident with a wavelength of $18\text{--}20 \mu\text{m}$ and an amplitude of $2\text{--}4 \mu\text{m}$. The profile normal to the wrinkles gives a root mean square (RMS) roughness of $2 \mu\text{m}$ and R_a value of $1.66 \mu\text{m}$ (Fig. 4(d)). To determine if the underlying PDMS has also wrinkled with the film, the Indium was etched out using 4-nitrophenol and NaOH solution. The resulting PDMS surface also showed wrinkles, indicating that the PDMS wrinkles along with the Indium film. However, it was difficult to establish if the Indium film remains fully bonded to the PDMS-Cr structure underneath during deformation, especially at the crest of the wrinkles. Furthermore, we were unable to establish a direct correlation between the Indium wrinkle patterns and the underlying cracked Chromium layer as the Indium film is not transparent to make these observations possible. Once the wrinkles are formed during the first cycle, significant strain can be obtained during subsequent loading simply by straightening them, thereby minimizing the need for plastic deformation during subsequent cycles. As discussed earlier, straightening of the wrinkles prevents an increase in ρ/ρ_0 during the initial stages of the second cycle, although in the latter stages it increases. It is hypothesized that one way to reduce the observed resistivity-rise during subsequent cycles would be to produce wrinkles of larger amplitude during the first cycle. This can be accomplished by placing the PDMS under tension during Indium deposition, and will be the subject of future work.

Below we discuss the possible mechanisms that allow the high stretch-ability of Indium films on PDMS (Figure 5(a)–5(c)).

- (i) In the un-stretched state, the Cr film, in its cracked state, strongly adheres with the PDMS on one side and Indium film on the other side (Fig. 5(a)).
- (ii) As PDMS is stretched, the Cr maintains its adhesion with the underlying PDMS as well as the overlying Indium film, and the Cr channel cracks widen to accommodate the deformation (Fig. 5(b)). The authors believe that the Indium layer is strained largely between the Cr-islands, with less strain accruing in the regions above the Cr-islands. The mechanism of strain accommodation needs to be further studied via in situ strain mapping during stretching in the SEM.
- (iii) The Indium film undergoes elastic-plastic deformation during stretching and yields at low stress and strain (at few MPa stress and $<2\%$ strain).³⁶ The necking instability of Indium is expected to be delayed if it is bonded well to a substrate.³³ Further studies are needed to identify if the Indium film recrystallizes or undergoes creep deformation since the T/T_m for Indium is about 0.69 at 25°C .

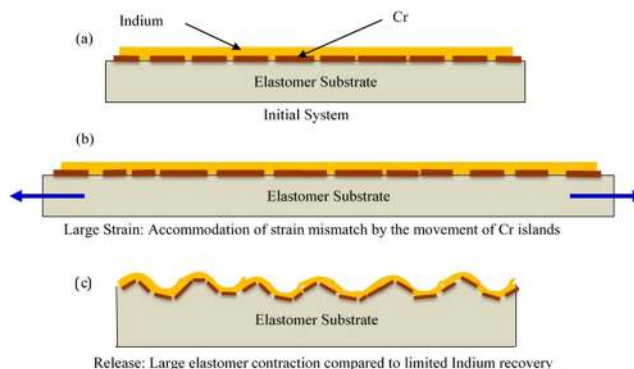


FIG. 5. Schematic of the mechanisms allowing the high stretch-ability of the Indium film over PDMS. (a) Indium film over PDMS with an interlayer of cracked Cr and (b) PDMS in stretched state. The widening of the Cr channels accommodates the deformation at the interface and (c) upon release of the strain, the PDMS undergoes large elastic and viscoelastic recovery, while the Indium film cannot recover the large plastic deformation accrued during loading. This incompatibility in the contraction leads to characteristic surface wrinkles.

(iv) Upon release of the strain, the PDMS shrinks to close to its original length via elastic recovery and viscoelastic deformation. The plastically extended Indium film cannot shrink as much, and therefore produces wrinkles on the surface to accommodate the contraction of PDMS (Figs. 4(b), 4(c), and 5(c)). The low stiffness of PDMS relative to In ($E_{\text{PDMS}} \sim 1.32\text{--}2.97$ MPa,⁴⁰ Elastic Modulus in tension ~ 12.74 GPa (Ref. 41)) makes its surface conform to the wrinkles in In, resulting in a wavy PDMS surface with the same periodicity as that of the In film (although it is unclear whether In film decoheres from the Cr/PDMS).

In summary, we have created highly stretchable Indium interconnect films on PDMS using cost effective methods such as PVD and electroplating. The level of stretch-ability of demonstrated in the current work without any geometric manipulations (e.g., creating helical or serpentine geometry) has not been reported to date. Further, the observation of the maximum strain of 70–100% without failure was limited by the failure of the PDMS substrate (see supplemental material³⁷ for a sample image after failure, Figure S1). As a result, the maximum strain to failure of the Indium film is as yet unknown. It is shown that the Cr islands over PDMS move away from each other while remaining strongly bonded to the PDMS under the high strain, providing adhesion and strain accommodation for the Indium film. The Indium film is shown to form surface wrinkles upon release from the large strain, confirming its strong adhesion to PDMS. These wrinkles reduce the need for plastic deformation during subsequent loading, thereby imparting additional stretch-ability during subsequent cycles. Resistance measurements during cyclic straining showed hysteresis in both resistance and the effective resistivity, both of which rose following cycling, possibly due to introduction or enlargement of defects. Further research is necessary to optimize the deposition conditions and microstructure to minimize this effect. We also note that the methods used in the current work are compatible with the processes used in the electronics industry, making these results important for the emerging areas of flexible electronics and wearable devices.

The authors gratefully acknowledge the assistance of Dr. L. Meinshausen, and Messrs. Md T. Rahman, Joshah Jennings, Robert Lentz, and Miles Pepper from the Washington State University with the experimental work. The work was supported by the startup funds for RP at WSU.

- ¹Y. Chen, J. Au, P. Kazlas, A. Ritenour, H. Gates, and M. McCreary, *Nature* **423**(6936), 136 (2003).
- ²G. H. Gelinck, H. E. A. Huitema, E. Van Veenendaal, E. Cantatore, L. Schrijnemakers, J. Van der Putten, T. C. T. Geuns, M. Beenhakkers, J. B. Giesbers, B. H. Huisman, E. J. Meijer, E. M. Benito, F. J. Touwslager, A. W. Marsman, B. J. E. Van Rens, and D. M. De Leeuw, *Nat. Mater.* **3**(2), 106–110 (2004).
- ³S. Kim, H. J. Kwon, S. Lee, H. Shim, Y. Chun, W. Choi, J. Kwack, D. Han, M. Song, S. Kim, S. Mohammadi, I. Kee, and S. Y. Lee, *Adv. Mater.* **23**(31), 3511 (2011).
- ⁴B. Yoon, D. Y. Ham, O. Yarimaga, H. An, C. W. Lee, and J. M. Kim, *Adv. Mater.* **23**(46), 5492 (2011).
- ⁵R. D. Ponce Wong, J. D. Posner, and V. J. Santos, *Sens. Actuators A: Phys.* **179**(0), 62–69 (2012).
- ⁶D. H. Kim, J. H. Ahn, W. M. Choi, H. S. Kim, T. H. Kim, J. Z. Song, Y. G. Y. Huang, Z. J. Liu, C. Lu, and J. A. Rogers, *Science* **320**(5875), 507–511 (2008).

- ⁷H. C. Ko, M. P. Stoykovich, J. Z. Song, V. Malyarchuk, W. M. Choi, C. J. Yu, J. B. Geddes, J. L. Xiao, S. D. Wang, Y. G. Huang, and J. A. Rogers, *Nature* **454**(7205), 748–753 (2008).
- ⁸D. H. Kim, N. S. Lu, R. Ma, Y. S. Kim, R. H. Kim, S. D. Wang, J. Wu, S. M. Won, H. Tao, A. Islam, K. J. Yu, T. I. Kim, R. Chowdhury, M. Ying, L. Z. Xu, M. Li, H. J. Chung, H. Keum, M. McCormick, P. Liu, Y. W. Zhang, F. G. Omenetto, Y. G. Huang, T. Coleman, and J. A. Rogers, *Science* **333**(6044), 838–843 (2011).
- ⁹N. M. Farandos, A. K. Yetisen, M. J. Monteiro, C. R. Lowe, and S. H. Yun, *Adv. Healthcare Mater.* **4**(6), 792–810 (2015).
- ¹⁰T. Someya, *Stretchable Electronics* (Wiley-VCH, Weinheim, 2013), p. 1 online resource (xxi, 462 pages).
- ¹¹R. Mahajan, P. Brofman, R. Alapati, C. Hilbert, L. Nguyen, K. Maekawa, M. Varughese, D. O'Connor, S. Ramaswami, and J. Candelaria, *Packaging Needs Document* (Semiconductor Research Corporation, 2015), pp 1–9.
- ¹²H. Yung-Yu, K. Lucas, D. Davis, B. Elolampi, R. Ghaffari, C. Rafferty, and K. Dowling, *IEEE Trans. Electron Devices* **60**(7), 2338–2345 (2013).
- ¹³Y.-Y. Hsu, M. Gonzalez, F. Bossuyt, F. Axisa, J. Vanfleteren, and I. De Wolf, *J. Micromech. Microeng.* **20**(7), 075036 (2010).
- ¹⁴R. Taylor, C. Boyce, M. Boyce, and B. Pruitt, *J. Micromech. Microeng.* **23**(10), 105004 (2013).
- ¹⁵Y. Zhang, H. Fu, Y. Su, S. Xu, H. Cheng, J. A. Fan, K.-C. Hwang, J. A. Rogers, and Y. Huang, *Acta Mater.* **61**(20), 7816–7827 (2013).
- ¹⁶Y. Zhang, S. Wang, X. Li, J. A. Fan, S. Xu, Y. M. Song, K. J. Choi, W. H. Yeo, W. Lee, and S. N. Nazaar, *Adv. Funct. Mater.* **24**(14), 2028–2037 (2014).
- ¹⁷Y.-Y. Hsu, M. Gonzalez, F. Bossuyt, F. Axisa, J. Vanfleteren, and I. De Wolf, *Thin Solid Films* **519**(7), 2225–2234 (2011).
- ¹⁸M. Jablonski, F. Bossuyt, J. Vanfleteren, T. Vervust, and H. de Vries, *Microelectron. Reliab.* **53**(7), 956–963 (2013).
- ¹⁹M. Gonzalez, B. Vandeveld, W. Christiaens, Y.-Y. Hsu, F. Iker, F. Bossuyt, J. Vanfleteren, O. Van der Sluis, and P. Timmermans, *Microelectron. Reliab.* **51**(6), 1069–1076 (2011).
- ²⁰C. Lv, H. Yu, and H. Jiang, *Extreme Mech. Lett.* **1**, 29–34 (2014).
- ²¹S. Béfahy, S. Yunus, T. Pardo, P. Bertrand, and M. Troosters, *Appl. Phys. Lett.* **91**(14), 141911 (2007).
- ²²J. A. Rogers, T. Someya, and Y. Huang, *Science* **327**(5973), 1603–1607 (2010).
- ²³E. Kim, H. Tu, C. Lv, H. Jiang, H. Yu, and Y. Xu, *Appl. Phys. Lett.* **102**(3), 033506 (2013).
- ²⁴D.-Y. Khang, H. Jiang, Y. Huang, and J. A. Rogers, *Science* **311**(5758), 208–212 (2006).
- ²⁵H. Yung-Yu, P. Cole, L. Daniel, W. Xianyan, R. Milan, Z. Baosheng, and G. Roozbeh, *J. Micromech. Microeng.* **24**(9), 095014 (2014).
- ²⁶S. Wagner and S. Bauer, *MRS Bull.* **37**(03), 207–213 (2012).
- ²⁷N. Lu, X. Wang, Z. Suo, and J. Vlassak, *J. Appl. Phys. Lett.* **91**(22), 221909 (2007).
- ²⁸Y. Xiang, T. Li, Z. Suo, and J. Vlassak, *J. Appl. Phys. Lett.* **87**(16), 161910 (2005).
- ²⁹S. P. Lacour, J. Jones, S. Wagner, T. Li, and Z. Suo, *Proc. IEEE* **93**(8), 1459–1467 (2005).
- ³⁰J. Jones, S. P. Lacour, S. Wagner, and Z. Suo, *J. Vacuum Sci. Technol. A* **22**(4), 1723–1725 (2004).
- ³¹O. Akogwu, D. Kwabi, S. Midturi, M. Eleruja, B. Babatope, and W. O. Soboyejo, *Mater. Sci. Eng.: B* **170**(1), 32–40 (2010).
- ³²T. Li and Z. Suo, *Int. J. Solids Struct.* **43**(7), 2351–2363 (2006).
- ³³T. Li, Z. Huang, Z. Xi, S. P. Lacour, S. Wagner, and Z. Suo, *Mech. Mater.* **37**(2), 261–273 (2005).
- ³⁴C. Tsay, S. P. Lacour, S. Wagner, T. Li, and Z. Suo, “How stretchable can we make thin metal films?,” in *MRS Proceedings* (Cambridge Univ Press, 2005), p O5. 5.
- ³⁵H. Vandeparre, Q. Liu, I. R. Mineev, Z. Suo, and S. P. Lacour, *Adv. Mater.* **25**(22), 3117–3121 (2013).
- ³⁶R. Reed, C. McCowan, R. Walsh, L. Delgado, and J. McColskey, *Mater. Sci. Eng.: A* **102**(2), 227–236 (1988).
- ³⁷See supplementary material at <http://dx.doi.org/10.1063/1.4929605> for sample image after failure, a histogram of strain-to-failure data, and a video of the stretching of one of the samples.
- ³⁸R. Hill, *The Mathematical Theory of Plasticity*, Oxford Classic Texts in the Physical Sciences (Oxford University Press, 1998).
- ³⁹N. Bowden, S. Brittain, A. G. Evans, J. W. Hutchinson, and G. M. Whitesides, *Nature* **393**(6681), 146–149 (1998).
- ⁴⁰I. Johnston, D. McCluskey, C. Tan, and M. Tracey, *J. Micromech. Microeng.* **24**(3), 035017 (2014).
- ⁴¹See <http://www.indium.com/metals/indium/physical-constants>, for “physical constants of pure indium by indium corporation,” (accessed 4 August).